Aqueous Ligand-Stabilized Palladium Nanoparticle Catalysts for Parahydrogen Induced ^{13}C Hyperpolarization

Jeffrey McCormick[a.b], Alexander M. Grunfeld[a], Yavuz N. Ertas[b,c], Akash N. Biswas[a], Kristofer L. Marsh[a], Shawn Wagner[d], Stefan Glöggler[a,e,f], Louis-S. Bouchard*[a,b,c]

[a]Department of Chemistry and Biochemistry, University of California at Los Angeles, 607 Charles E Young Drive East, Los Angeles, California 90095-1569, USA

[b]The Molecular Biology Institute, Jonsson Comprehensive Cancer Center, California NanoSystems Institute (CNSI), University of California Los Angeles, Los Angeles, CA 90095, USA

[c]Department of Bioengineering, University of California at Los Angeles, 607 Charles E Young Drive East, Los Angeles, California 90095-1569, USA

[d]Biomedical Imaging Research Institute, Cedars Sinai Medical Center, 8700 Beverly Blvd, Davis Building G149E, Los Angeles, California 90048, USA

[e]Max Planck Institute for Biophysical Chemistry, Am Fassberg 11, D-37077 Göttingen, Germany

[f]Center for Biostructural Imaging of Neurodegeneration, Von-Siebold-Str. 3A, D-37075 Göttingen, Germany

Corresponding Author
*Professor Louis Bouchard
louis.bouchard@gmail.com

SUPPORTING INFORMATION TABLE OF CONTENTS

S1 MATERIALS AND METHODS

CHEMICALS AND SUPPLIES

Palladium chloride, 99% ($PdCl_2$), sodium borohydride, L-cysteine (LCys), N-acetyl-L-cysteine (NAC) and DL-propargylglycine were purchased from Sigma Aldrich and used without further modification. Solvents for purification such as n-hexanes, anhydrous isopropanol and anhydrous, absolute ethanol were purchased from Fisher Scientific and used as received, unless degassed as mentioned by freeze-pump-thaw. MilliQ water was generated by in house filtration and collected at ≥ 17.8 MΩ resistance. Deuterated solvents (D_2O and $CDCl_3$) were purchased by Cambridge Isotope Laboratories and used as received. Degassed solvents were prepared by no less than three freeze-pump-thaw cycles of submerging in liquid nitrogen, pulling static vacuum for ~30 minutes, and slowly thawing in a water bath before allowing nitrogen flow.

NANOPARTICLE AND LIGAND CHARACTERIZATION

NMR measurements were recorded on a Bruker AV600 system using a 5 mm broadband probe. Thermogravimetric analysis (TGA) of nanoparticle ligand coverage was measured using a Perkin Elmer Pyris Diamond TG/DTA in alumina pans spanning from 25°C to 700°C under argon flow at 5 °C/min. Transmission electron microscopy (TEM) was performed using an FEI Tecnai T12 microscope after suspension of nanoparticles in MilliQ water and drying on carbon substrate grids before imaging. X-ray photoemission spectroscopy (XPS) studies were carried out on a Kratos AXIS Ultra DLD X-ray photoelectron spectrometer with a monochromatic Al Kα X-ray source operating at 10 mA and 15 kV. UV/Vis characterization spectra were collected on an Agilent 8453 UV-Vis spectrometer from 190 nm to 800 nm. Centrifugation was performed on a Beckman Avanti J-25 using a JA-14 rotor. Inert chemistry was conducted using standard Schlenk technique under nitrogen flow.

S2 SYNTHETIC PROCEDURES

INERT SYNTHESIS OF L-CYSTEINE-CAPPED PALLADIUM NANOPARTICLES (LCYS@PD)

Inert synthesis conditions were heavily modified from previously published work[1]. 177 mg of $PdCl_2$ (1 mmol) was added to a 500 mL flask under argon atmosphere before addition of 99 mL degassed MilliQ water and 1 mL of aqueous 2M HCl solution stirred at 360 RPM under nitrogen flow overnight to produce 10 mM H_2PdCl_4 metallic acid precursor. In a separate flask, 121 mg L-cysteine (1 mmol) was dissolved in 27.5 mL degassed MilliQ water and added into the H_2PdCl_4 solution quickly. Addition of the ligand solution causes immediate color change from transparent brown H_2PdCl_4 to cloudy orange H_2PdCl_4:LCys complex characterized by UV/Vis in this work. After stirring for 1 hour, a fresh solution of 377 mg $NaBH_4$ (10 mmol) was prepared in 15 mL degassed MilliQ water, and added to the H_2PdCl_4:LCys dropwise over 4 minutes. Introduction of $NaBH_4$ causes immediate color change to black, indicating reduction into nanoparticles. Freshly formed nanoparticles were left to stir overnight before solvent fractionation by addition of 107 mL isopropanol and 53 mL *n*-hexanes for 8 hours stirring at 360 RPM. Solution was balanced and centrifuged at 6000 RPM (5509xg) for 25 minutes. Supernatants were discarded and pellet was washed 4x with absolute ethanol before drying under static vacuum.

INERT SYNTHESIS OF N-ACETYLCYSTEINE-CAPPED PALLADIUM NANOPARTICLES (NAC@PD)

177 mg of $PdCl_2$ (1 mmol) was added to a 500 mL flask under argon atmosphere before addition of 99 mL degassed MilliQ water and 1 mL of aqueous 2M HCl solution stirred at 360 RPM under nitrogen flow overnight to produce 10 mM H_2PdCl_4 metallic acid precursor. In a separate flask, 163 mg N-acetylcysteine (1 mmol) was dissolved in 27.5 mL degassed MilliQ water and added into the H_2PdCl_4 solution quickly. Addition of the ligand solution causes immediate color change from transparent brown H_2PdCl_4 to transparent pink H_2PdCl_4:NAC complex. After stirring for 1 hour, a fresh solution of 377 mg $NaBH_4$ (10 mmol) was prepared in 15 mL degassed MilliQ water, and added to the H_2PdCl_4:NAC dropwise over 4 minutes. Introduction of $NaBH_4$ causes immediate color change to black, indicating reduction into nanoparticles. Freshly formed nanoparticles were left to stir overnight before solvent fractionation by addition of 225 mL isopropanol and 53 mL *n*-hexanes for 8 hours stirring at 360 RPM. 225 mL isopropanol was found to fractionate the NAC@Pd nanoparticles best for high polarization. The solution was balanced and centrifuged at 6000 RPM (5509xg) for 25 minutes. Supernatants were discarded and pellet was washed 4x with absolute ethanol before drying under static vacuum.

AIR SYNTHESIS OF LCYS@PD AND NAC@PD NANOPARTICLES

Synthesis of NAC@Pd and LCys@Pd nanoparticles in open air were performed using identical preparation, mixing and purification procedures in Erlenmeyer flasks and an open 500 mL round bottom flask without nitrogen flow. Although XPS in this work identifies higher oxidation of surface palladium (see Fig. S6), ^{1}H polarization experiments performed using LCys@Pd nanoparticles prepared inertly and in open air show no significant difference in polarization.

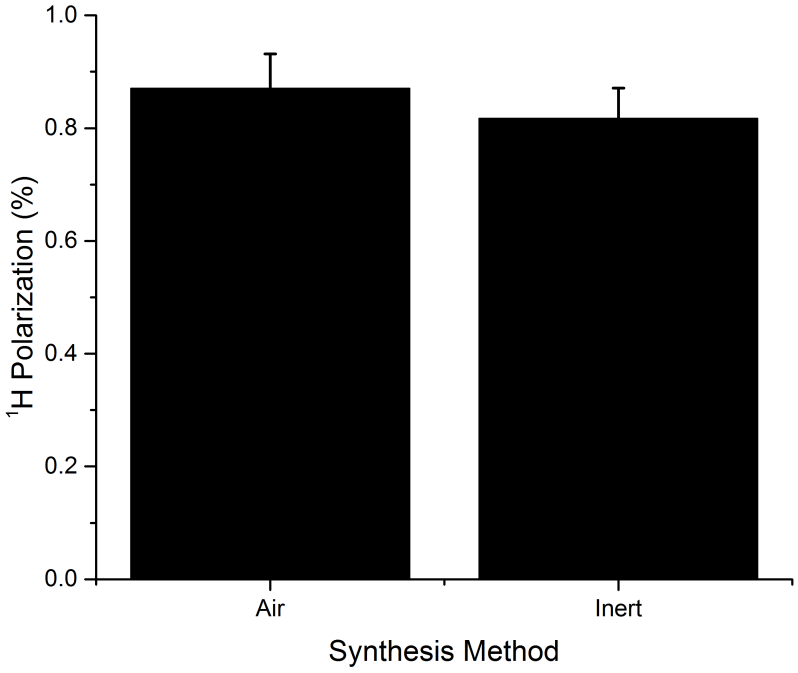

Figure S1. ^{1}H polarization experiments repeated over three trials using 10 mg/mL LCys@Pd nanoparticles with 2-hydroxyethyl acrylate (HEA) at 80°C show no polarization loss, if not slight benefit, from open air synthesis.

S3 NANOPARTICLE CHARACTERIZATION

$PD^{(II)}$ TO PD^0 CONVERSION DURING NANOPARTICLE FORMATION

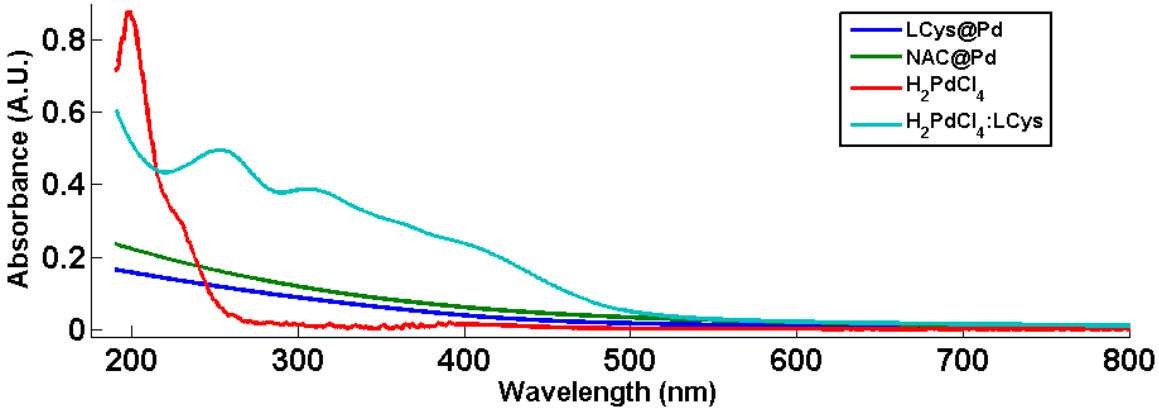

Figure S2. UV/Vis spectra of aqueous solutions throughout nanoparticle synthesis from 180-800 nm.

Figure S2 shows the UV/Vis spectra of aqueous H_2PdCl_4 solution, H_2PdCl_4:amino acid complex, and both LCys@Pd and NAC@Pd in water. Broad absorbance bands at around 410 nm are attributed to metal-to-ligand charge transfer[2], while the shoulder band and sharp peak at 228 nm and 205 nm respectively represent ligand-to-metal charge transfer[3]. Introduction of stabilizing ligand (LCys shown) causes collapse of the 228 nm, 207 nm and 410 nm and instead a prominent absorption band at around 260 nm appears, which can be assigned to a S–$Pd^{(II)}$ charge transfer band upon complexation with cysteine thiolate[3]. Upon reduction of the H_2PdCl_4:amino acid solution, ionic $Pd^{(II)}$ absorption bands disappear, and product nanoparticle solutions show only scarce scattering characteristic of colloid solutions, indicating removal of dissolved Pd ions. Ligand coordination was also confirmed by ^{1}H NMR spectra indicating line broadening due to surface interaction (see Fig. S5).

TRANSMISSION ELECTRON MICROSCOPY (TEM) OF LCYS@PD AND NAC@PD PARTICLES

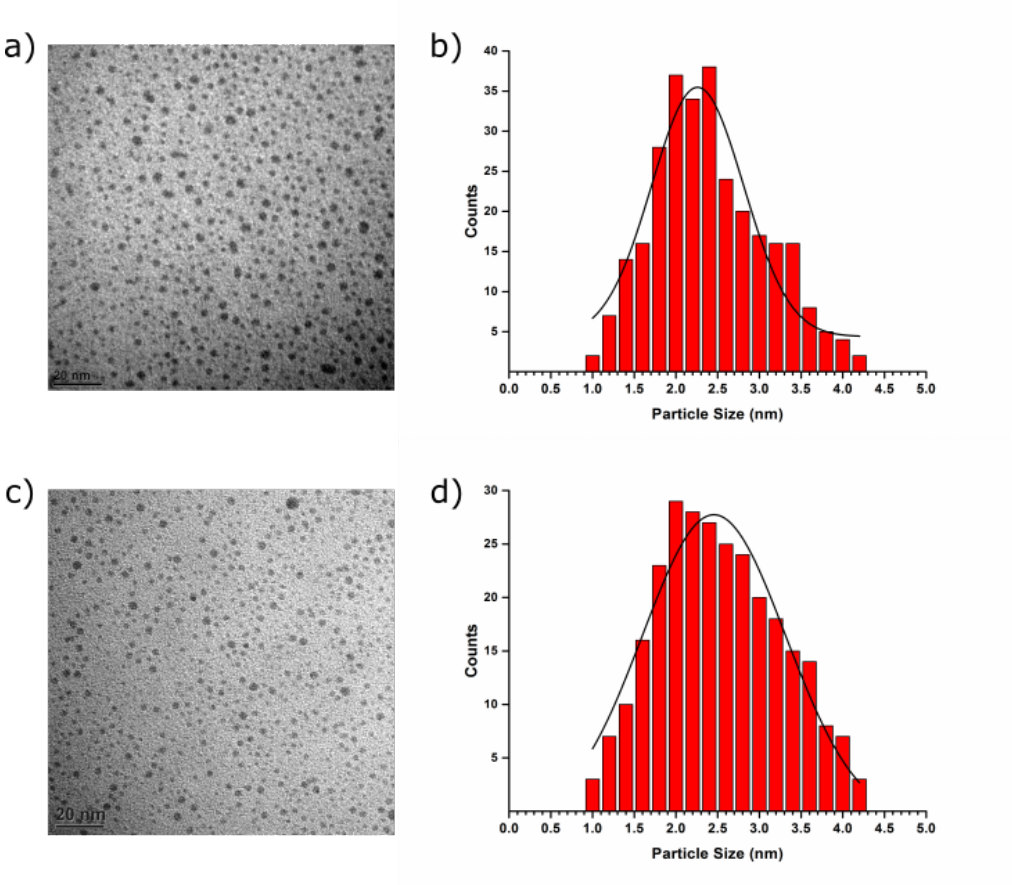

Figure S3. a) TEM image of NAC@Pd nanoparticles dried after dispersion in water. c) TEM image of LCys@Pd nanoparticles dried after dispersion in water. Size distributions for NAC@Pd and LCys@Pd are shown in b) and d), respectively.

For LCys@Pd and NAC@Pd nanoparticles, 277 and 288 particles were chosen at random and compiled into the size distributions shown in Fig S3 b) and d) respectively. Particle sizes of 2.4 ± 0.6 nm and 2.5 ± 0.8 nm were found for NAC@Pd and LCys@Pd, respectively. Deviations were calculated from the Gaussian fits shown in Fig. S3.

THERMOGRAVIMETRIC ANALYSIS (TGA)

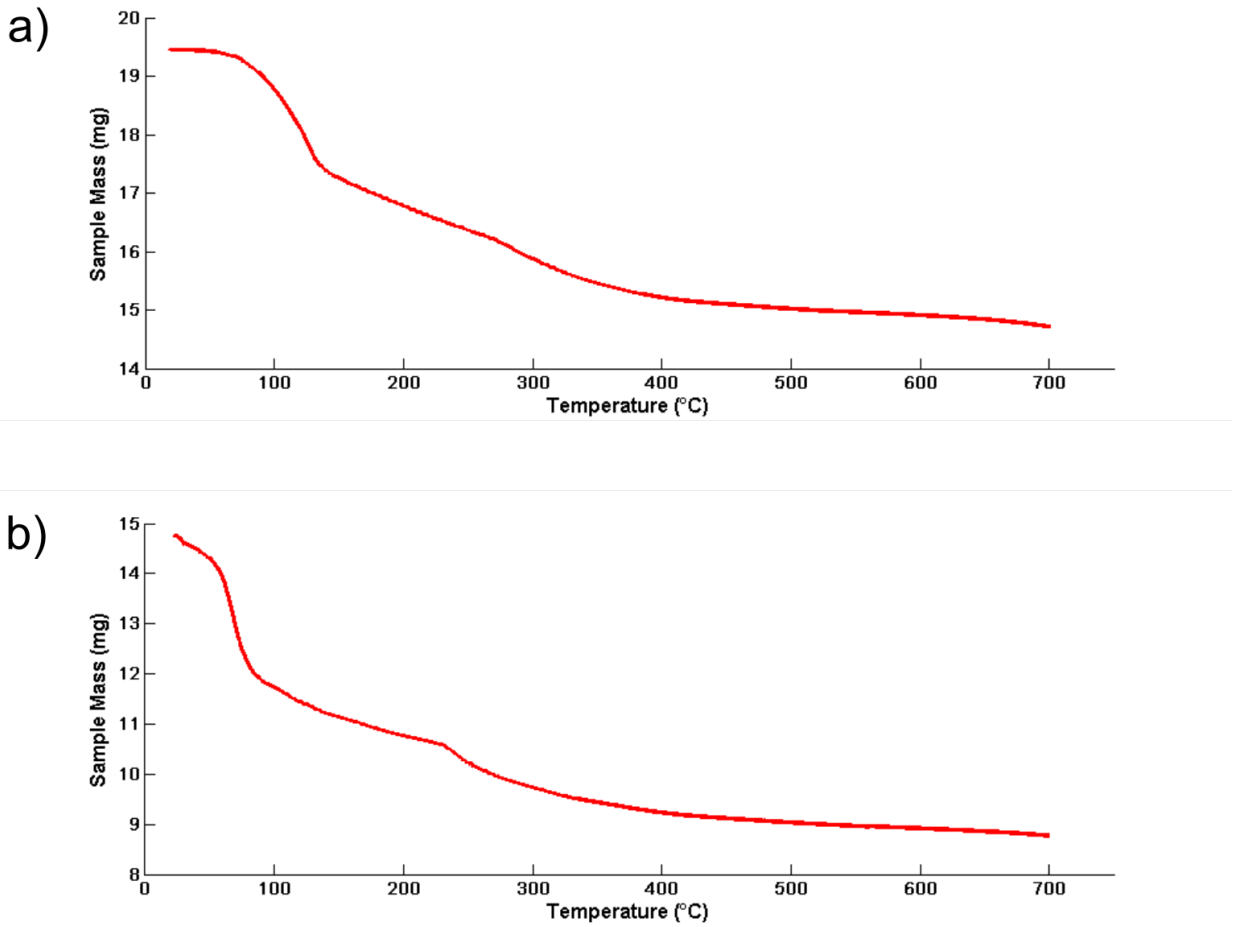

Figure S4. TGA curves of a) NAC@Pd and b) LCys@Pd particles under argon flow. Organic decomposition of the ligand increases with temperature until ≥650°C, after which no appreciable mass change is observed.

Thermogravimetric Analysis (TGA) is used to characterize ligand coverage of different heterogeneous nanoparticle systems. Decomposition of ligand in Fig. S4 indicates 25% ligand coverage of LCys@Pd and 40% coverage of NAC@Pd particles, potentially contributing to their ability to perform pairwise para-H_2 addition during hydrogenation.

CHARACTERIZATION OF LIGAND COORDINATION BY NMR

To demonstrate ligand coordination to the surface of the nanoparticles, ^{1}H NMR spectra were collected on a Bruker 600 MHz spectrometer to identify line broadening in the presence of nanoparticles. Dipolar peak broadening of both LCys@Pd and NAC@Pd suspensions particles indicate surface coordination.

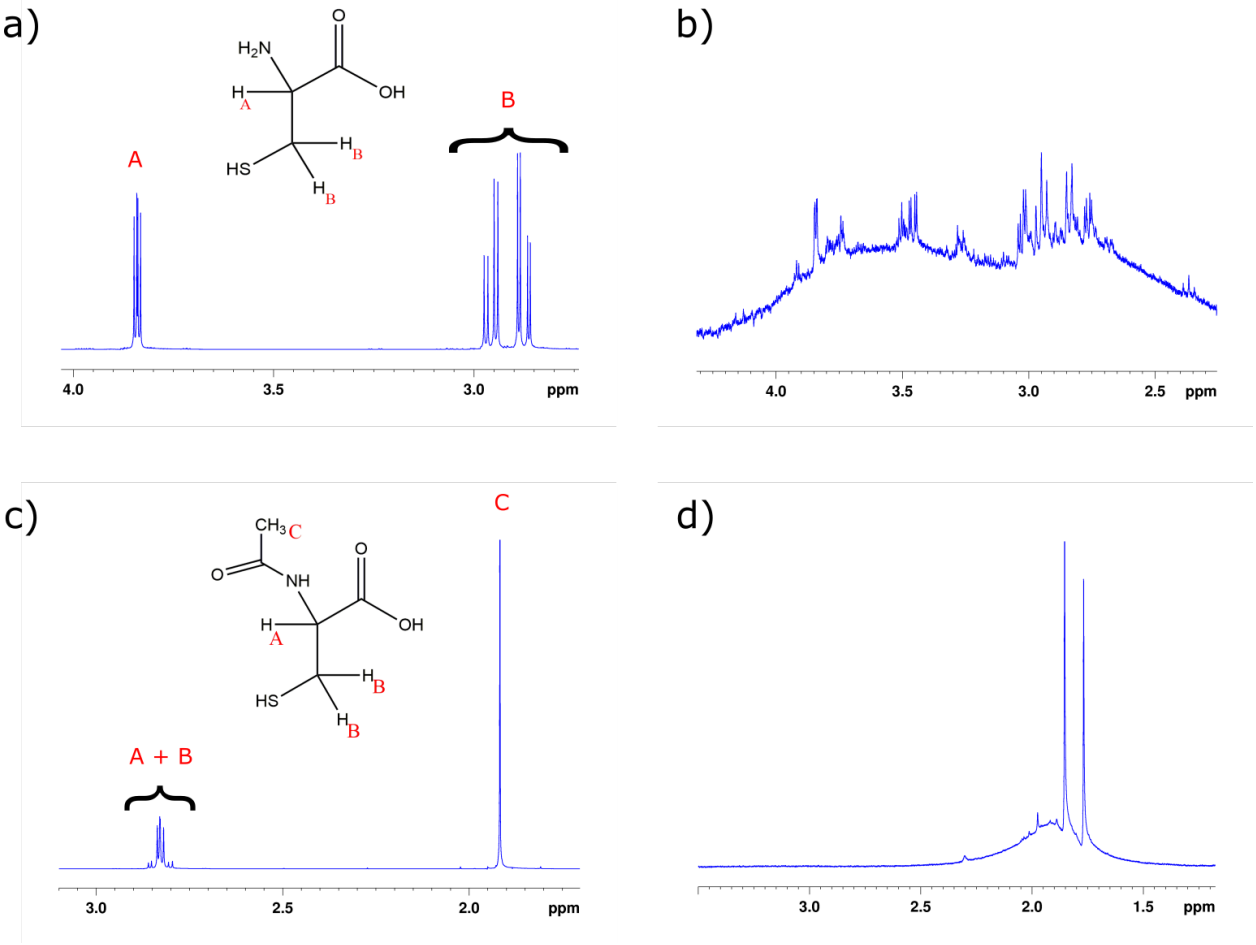

Figure S5. ^{1}H NMR spectra of a) L-cysteine ligand and b) LCys@Pd dissolved in D_2O. Broadening of ligand peaks in b) indicates significant coordination of ligand to metal. A similar broadening is observed for c) N-acetylcysteine and d) NAC@Pd nanoparticles dissolved in D_2O.

X-RAY PHOTOELECTRON SPECTROSCOPY (XPS) OF PD OXIDATION

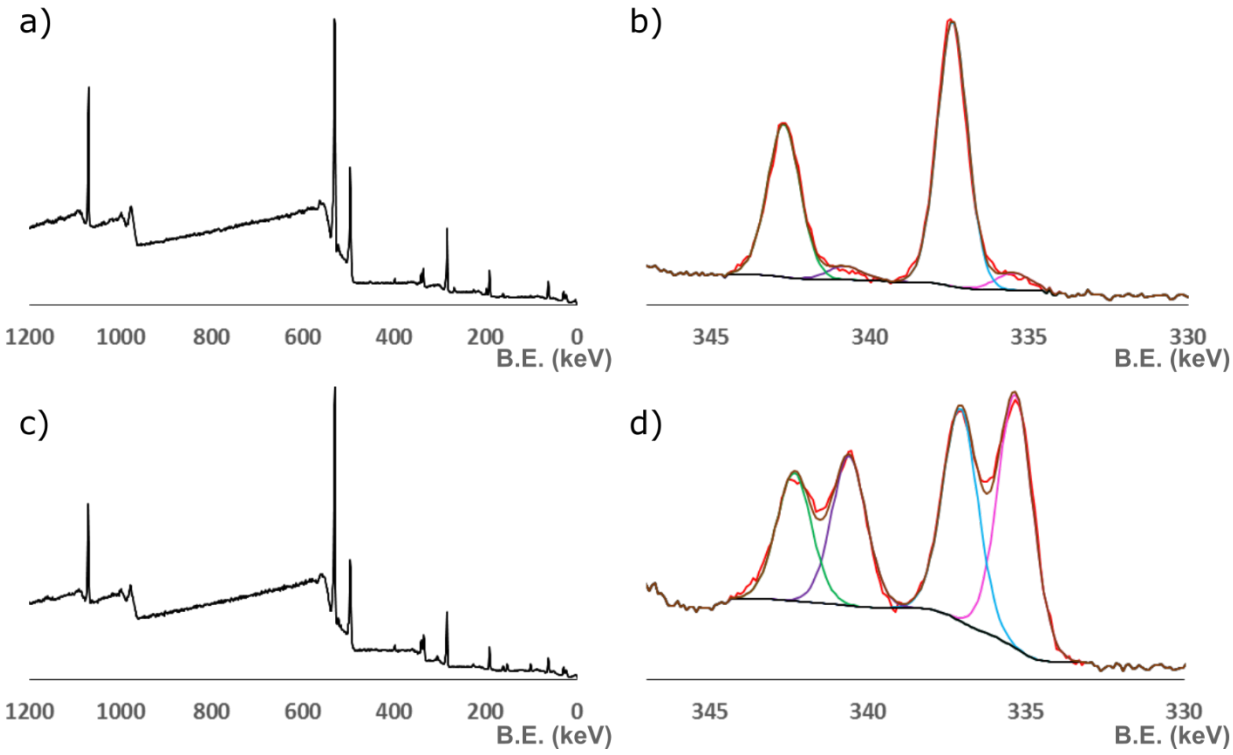

Figure S6. XPS spectra. The a) survey and corresponding b) Pd 3d hi-resolution spectrum of LCys@Pd synthesized under inert conditions. Air-synthesized c) survey and d) Pd 3d spectra are shown for comparison of Pd oxidation.

XPS studies were performed on a Kratos AXIS Ultra DLD X-ray photoelectron spectrometer with a monochromatic Al Kα X-ray source operating at 10 mA and 15 kV. Survey spectra and individual high-resolution spectra were collected using pass energies of 160 eV and 20 eV, respectively. Data processing was performed using CasaXPS 2.3 software, and spectral binding energies were calibrated by assigning the hydrocarbon peak in the C 1s high-resolution spectra, as a result of adventitious carbon, to 284.6 eV. It is clear from observation of the hi-resolution XPS spectra (Fig. S6) that the palladium particles synthesized in open air have much higher oxidized Pd content than those formed under inert chemistry. The Pd $3d_{5/2}$ peak at approximately 335.3 eV is assigned to palladium metal, whereas the Pd $3d_{5/2}$ peak at 337.1 eV is assigned to the native oxide[4].

S4 PARAHYDROGEN-INDUCED POLARIZATION (PHIP) EXPERIMENTS

EXPERIMENTAL PROCEDURE

^{1}H and ^{13}C NMR spectra for PHIP experiments were performed on a Bruker AV600 spectrometer at B_0 = 14.1 T. Solutions were prepared in 5 mm J-Young tubes purchased from New Era. Under inert conditions, nanoparticles were suspended in degassed D_2O before adding 4 µL (0.04 mmol) 2-hydroxyethyl acrylate (HEA), or 4 mg DL-propargylglycine (0.04 mmol) and 550 µL of the resulting mixture was added into a J-young tube and sealed. Samples were heated to 80°C before pressurizing with 80 PSI para-H_2 at Earth's field, before shaking vigorously in transit to be inserted into the high-field spectrometer bore, in accordance with previously reported ALTADENA PHIP conditions[5,6]. For ^{13}C transfer experiments, samples were pressurized and shaken before quick insertion into a three concentric cylinder µ-metal shield (Magnetic Shield Corp.) and drawn out slowly before transit. HEP products showed highest polarization with a 2 second draw, whereas EA products showed highest polarization at 5 second draw. Transit time was recorded at 9 seconds. PHIP spectra were then recorded with a single $45°_x$ ^{1}H pulse, or $90°_x$ ^{13}C proton-decoupled pulse. Reactions are then allowed several T_1 relaxation times to reach thermal polarization. Signal enhancement and its resulting polarization are calculated by comparing the integrals of hyperpolarized and thermal peaks. Thermal ^{13}C spectra were acquired using 256 scans, waiting 5 x T_1 between scans.

CONCENTRATION DEPENDENCE OF NAC@PD AND LCYS@PD NANOPARTICLES

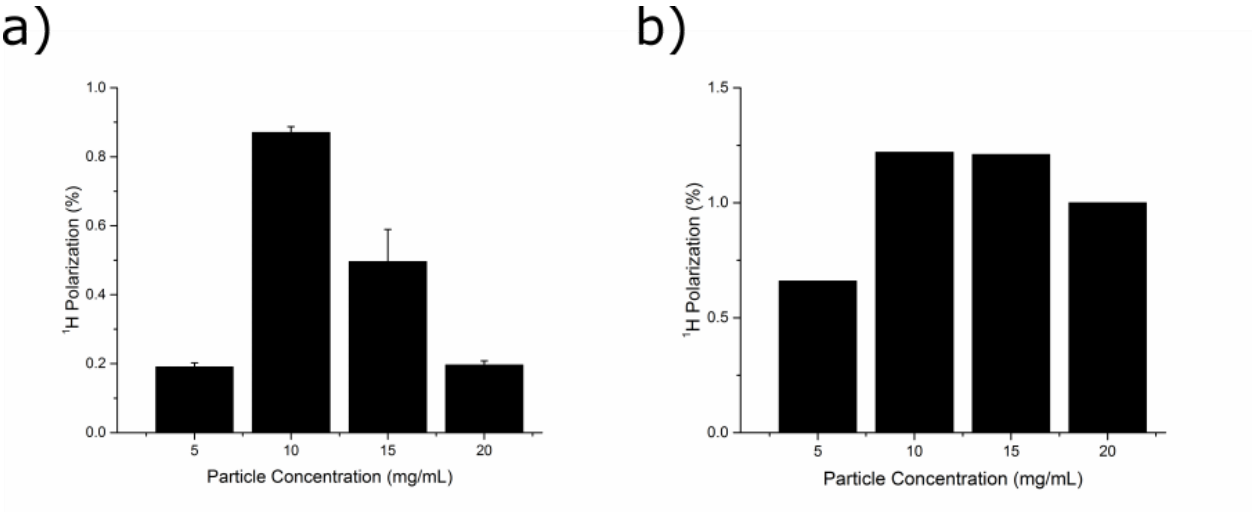

Figure S7. ^{1}H polarization of HEP measured by PHIP experiments at 80°C and 80 PSI of a) LCys@Pd and b) NAC@Pd nanoparticles.

Particle concentration experiments were performed by measuring ^{1}H polarization values using HEP formation at different particle concentrations. For both LCys@Pd and NAC@Pd, 10 mg/mL displayed the highest polarization.

S5 NANOPARTICLE RECOVERY

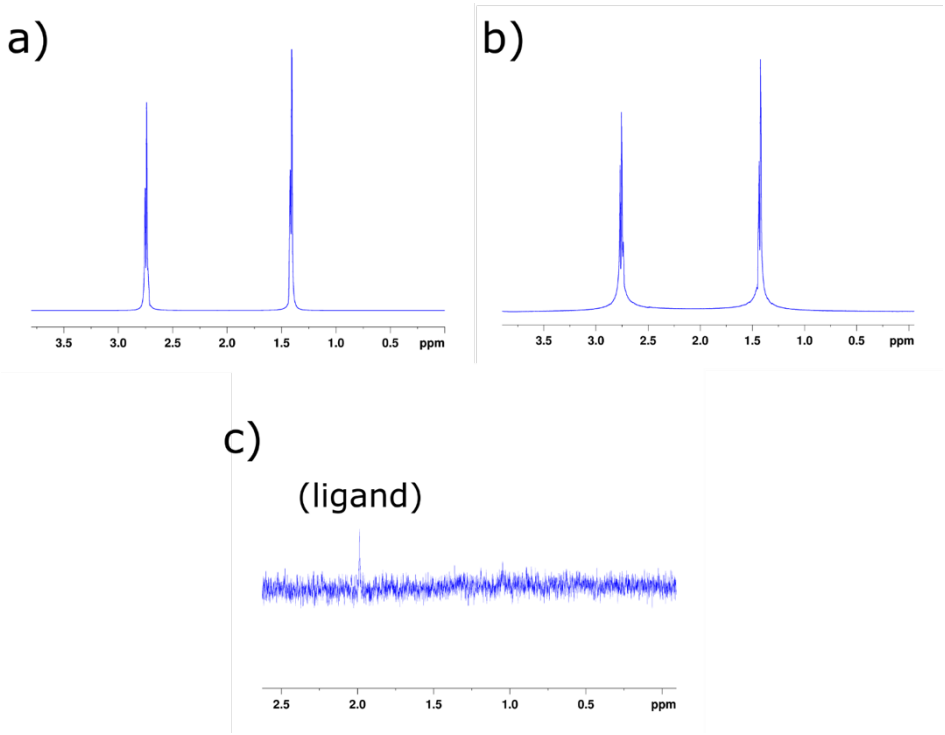

Figure S8. ^{1}H PHIP spectra of HEA hydrogenation in D_2O acquired after pressurizing a) fresh 20 mg/mL LCys@Pd nanoparticles, b) recycled nanoparticle pellet, and c) recycled supernatant solution with para-H_2. Spectra are acquired in a single 45° pulse and displayed in magnitude mode.

To further demonstrate the heterogeneous nature of catalysis involved in hydrogenation and its resulting hyperpolarization, as well as catalyst separation, PHIP experiments were designed to show conversion of 2-hydroxyethyl acrylate (HEA) using nanoparticles before and after their removal. 20 mg/mL LCys@Pd were suspended in degassed D_2O with 0.04 mmol HEA, pressurized to 80 psi para-H_2 at 80°C, and shaken before measurement with a single 45° ^{1}H pulse. The suspension was then removed and added to an excess of ethanol, causing nanoparticles to precipitate out. This solution was then spun by centrifugation at 10,000xg for 30 minutes. The nanoparticle pellet was rinsed briefly with ethanol before drying under static vacuum, while the supernatant was transferred to a new vial and centrifuged again for 30 minutes at 10,000xg before drying the final supernatant. Both supernatant and pellet products were resuspended in 550µL of degassed D_2O with fresh HEA added, and PHIP experiments were carried out as previously mentioned. PHIP spectra are shown in Fig. S8 revealing recovery of PHIP signal using separated the nanoparticle pellet, and undetectable product peaks using supernatant solution even under PHIP settings. This indicates that both the conversion and hyperpolarization methods described are heterogeneous with no indication of free Pd^{2+} ion contribution detectable, a crucial advantage of our system.

S6 REFERENCES

[1] S. Sharma, B. Kim, D. Lee, *Langmuir* **2012**, *28*, 15958–65.
[2] S. Nath, S. Praharaj, S. Panigrahi, S. K. Ghosh, S. Kundu, S. Basu, T. Pal, *Langmuir* **2005**, *21*, 10405–8.
[3] T. Harada, S. Ikeda, M. Miyazaki, T. Sakata, H. Mori, M. Matsumura, *J. Mol. Catal. A Chem.* **2007**, *268*, 59–64.
[4] W. Zhang, H. Huang, F. Li, K. Deng, X. Wang, *J. Mater. Chem. A* **2014**, *2*, 19084–19094.
[5] S. Glöggler, A. M. Grunfeld, Y. N. Ertas, J. McCormick, S. Wagner, P. P. M. Schleker, L. S. Bouchard, *Angew. Chemie - Int. Ed.* **2015**, *54*, 2452–2456.
[6] S. Glöggler, A. M. Grunfeld, Y. N. Ertas, J. McCormick, S. Wagner, L. S. Bouchard, *Chem. Commun.* **2016**, *52*, 605–608.